[redacted]

NRL REPORT 3529

FR-3529

THE THERMAL DISCONTINUITY AT THE HORIZON OBSERVED FROM HIGH ALTITUDES

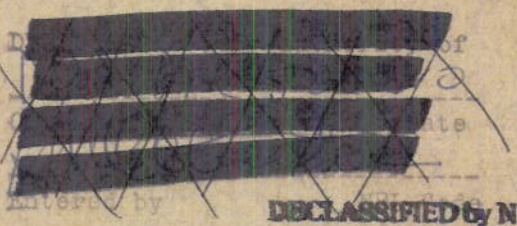

NAVAL RESEARCH LABORATORY

WASHINGTON, D.C.

NRL REPORT 3529

THE THERMAL DISCONTINUITY AT THE HORIZON OBSERVED FROM HIGH ALTITUDES

C. F. Bieber and H. L. Clark

September 12, 1949

Approved by:

J. A. Sanderson, Superintendent (Acting), Optics Division

NAVAL RESEARCH LABORATORY

CAPTAIN F. R. FURTH, USN, DIRECTOR

WASHINGTON, D.C.

DISTRIBUTION

CNO	1
ONR	
Attn: Code 421	15
BuAer	
Attn: EL-71 EL-81 2	5
Attn: Code TD-4 EL-84 2	1
BuOrd	
Attn: Code Re4e	10
Attn: Code Re9d	2
BuShips	
Attn: Code 841	10
Dir., USNEL	2
CDR., USNOTS	
Attn: Reports Unit	2
CO, USNUSL	
Attn: Infrared Division	2
OCSigO	
Attn: Ch. Eng. & Tech. Div., SIGTM-S	1
CO, SCEL	
Attn: Dir. of Engineering	2
CO, ERDL, Ft. Belvoir	
Attn: Mr. O. P. Cleaver	1
Dir., ESL	1
CG, AMC, Wright-Patterson AFB	
Attn: Dr. P. Overbo	1
Attn: Eng. Div., Electronics Subdiv., MCREEO	1
CO, Air Force Cambridge Res. Labs.	
Attn: ERRS	1
CO, Watson Labs., AMC, Red Bank	
Attn: ENR	1
BAGR, CD, Wright-Patterson AFB	
Attn: CADO-D1	1
Supt., US Naval Observatory, Wash., D. C.	
Attn: Mr. J. S. Hall	1
RDB	
Attn: Library	2
Attn: Navy Secretary	1
Attn: Guided Missiles Committee	2
Naval Res. Sec., Science Div., Lib. of Congress	
Attn: Mr. J. H. Heald	2

CONTENTS

ABSTRACT

In long-range, high-altitude, missile-guidance systems utilizing automatic celestial navigation, one of the problems encountered is the establishment of a stable vertical in relation to the earth. A possible method for determining the position of the vertical is to bisect the angle formed at the missile by optical paths which extend from two arbitrary points diametrically situated on the horizon. Previous measurements made at low altitudes had indicated that the horizon is sharply defined by a thermal radiation discontinuity. Similar measurements were conducted at high altitudes to determine whether the same discontinuity exists.

Thermal radiation signals, resulting from sweeping the field of view of an airborne optical system vertically across the natural horizon, were observed during daylight and darkness from altitudes of 2200 to 30,000 feet. From the resulting data, the apparent radiation temperatures and the thermal radiation gradients of the sky and land background were obtained. The existence of a sharp thermal radiation discontinuity at or near the horizon viewed from these altitudes, was established by the thermal gradient characteristics. Low-hanging clouds, which extended from just above the horizon to over 50,000 feet, produced signals similar to those from the horizon. Both the angular error in determining the position of the horizon and the cloud interference can be reduced by proper design of the optical system.

The use of the thermal radiation discontinuity at the horizon appears promising for establishing the vertical in guided-missile navigation systems.

PROBLEM STATUS

This report concludes work on the problem. Unless otherwise notified, the Laboratory will consider the problem closed one month from the mailing date of this report.

AUTHORIZATION

NRL Problem N03-17R
(NR 473-170)

THE THERMAL DISCONTINUITY AT THE HORIZON OBSERVED FROM HIGH ALTITUDES

INTRODUCTION

In long-range, high-altitude, missile-guidance systems utilizing automatic celestial navigation, one of the problems encountered is the establishment of a stable vertical in relation to the earth. A possible method for determining the position of the vertical is to bisect the angle formed at the missile by optical paths which extend from two arbitrary points diametrically situated on the horizon. Previous measurements made at sea level and at low altitudes,[1,2] particularly those concerned with thermal radiation gradients,[3,4] have indicated that the horizon is sharply defined by a thermal-radiation discontinuity which is present during both day and night. It is the purpose of NRL Problem No. 3-17R to determine whether a similar thermal discontinuity exists when the horizon is viewed from high altitudes and, if so, the characteristics of the discontinuity.

The necessary equipment was assembled by this Laboratory in December 1948. It was not, however, until the latter part of April 1949, after several postponements, that a B-29 aircraft was made available to the Laboratory at NOTS, Inyokern, California, for equipment installation and test. During the ensuing period of one month, 20 hours of flying time were made available. Consequently only three flights in all, two in daylight and one at night, were completed. All flights were made over the southern portion of California.

By scanning vertically across the horizon with an optical system containing a radiation thermopile, both the radiation temperatures and the thermal radiation gradients in the vicinity of the horizon were observed. From the characteristics of the thermal gradient, it was established that a thermal radiation discontinuity exists at the horizon when observed at altitudes up to 30,000 feet. The edges of clouds, observed to exist as high as 50,000 feet, also gave signals similar to those from the horizon. By properly designing the optical system, however, the error in determining the angular position of the horizon and

---

[1] *Sanderson, J. A., Lamberson, F. D., and Smith, P. S., "Radiation Temperatures of the Sky and the Sea Horizon," NRL Memo S-S70-4(1)(422) (Restricted), April 17, 1944*

[2] *Meyers, V. W. and Smith, P. S., "The Radiation Temperature of the Sky and Sea Horizon," NRL Report H-2505 (Restricted), April 18, 1945*

[3] *Clark, H. L, "Measurement of Thermal Gradients at the Horizon," BuShips Electrical Section Report No. 7, (Secret) September 15, 1944*

[4] *Summary Technical Report of Division 16, NDRC Volume 3 (Nonimage Forming Infrared), Section 9.3.3, pp. 288-289 (Confidential).*

the interference from clouds can be reduced, thus making this method of establishing the vertical rather promising.

It should be pointed out that these first measurements are purely exploratory and that they are an attempt to find a yes or no answer, quickly and at not too great expense. Exact measurements will require equipment designed specifically for the purpose and based in part on the findings reported here.

EQUIPMENT

An assembly was made using, as far as possible, existing components in order to save the time ordinarily required to design and fabricate special gear. This consisted of (1) the optical head of a Mark III Passive Bearing Finder System,[5] (2) a Perkin-Elmer d-c breaker amplifier, (3) a low-pass filter, (4) a direct-coupled amplifier, and (5) a dual-channel Brush Oscillograph. A block diagram of the system is shown in Figure 1.

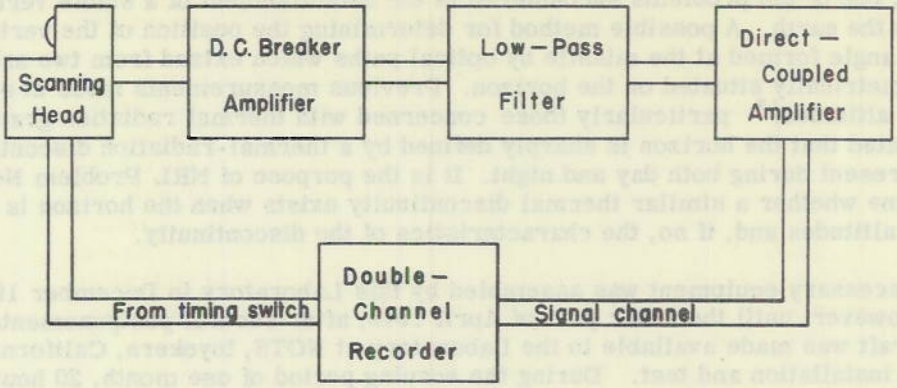

Figure 1 - Block diagram of system

The optical head employed an f/0.67, 3-inch-diameter catadioptric optical system of the mirror-meniscus type, in which the spherical mirror and the thermopile were integrally mounted (Figure 2). A total angle of 16.5 degrees was scanned vertically, at a rate of 20 cycles per minute, by rotation of the mirror-thermopile assembly about an axis through the center of curvature of the meniscus.*

A special mount, incorporating an ordinary 6 x 30 prism monocular placed at the side of the scanner to serve as a pressure-tight observation window, was constructed to maintain

---

[5] *Farrand Optical Company Service and Operating Instructions for PBF Mod. 3 (Confidential).*

* *Anticipating the conditions under which this mechanism would be required to operate, preliminary tests were conducted with the scanner operating inside a high-altitude chamber where pressure and temperature could be varied at will. Because of the low temperature, it was found necessary to remove the original lubricant and replace it with a special low-temperature lubricant developed by the Lubrication Branch, Chemistry Division of this laboratory. This change permitted the scanner to continue operating in a normal manner after it had been held at -50°C for a period of thirty minutes.*

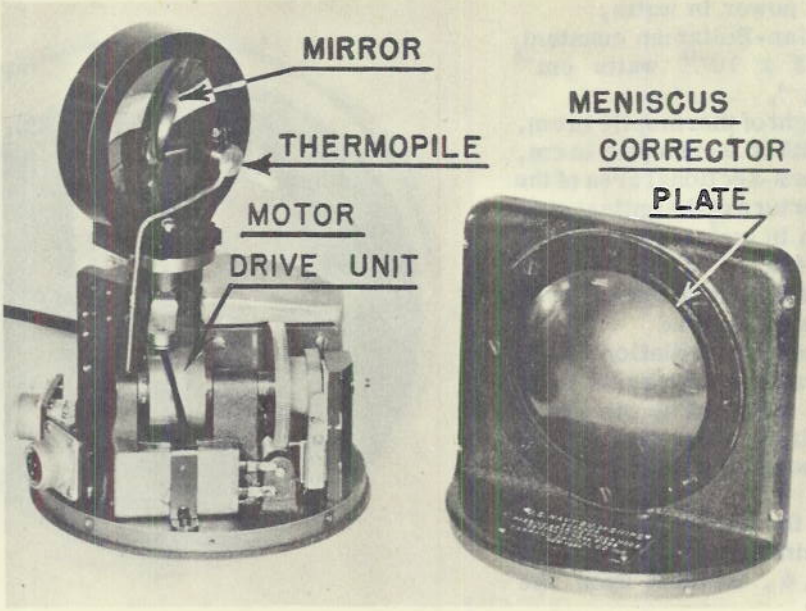

Figure 2 - Scanner mechanism and optical system

the axis of the scanner in a horizontal position (thereby allowing the optical field of view to sweep vertically across the horizon) and to provide a pressure seal which allowed the back to be taken off the head and the thermopile half-cover put in place or removed as desired without permitting air to escape from the aircraft's pressurized cabin.

A filter (Figure 3; transmission curve, Figure 4), mounted in front of the meniscus corrector plate, prevented visible light from entering the system.

Two Harris[6] compensated thermopiles (identical halves connected in electrical opposition), of dimensions which defined a field of view 3/4 degree-3/4 degree-3/4 degree high by 3 degrees wide (Figure 5), were used for the tests. When such a thermopile views an extended target of uniform temperature, no signal is generated. However, when one half views a target of an apparent temperature differing from that viewed by the other half, a signal is generated which is proportional to difference in radiation falling on the two halves of the thermopile. In other words, the thermopile responds to any thermal gradient present in the target being viewed.

If one half of the thermopile is kept covered and the mask is maintained at a fixed temperature, the system indicates the difference between the radiation received from the target by the uncovered half of the thermopile and the constant radiation from the mask over the covered portion. That is to say, the thermopile then responds to the absolute magnitude of the radiation from the target.

Mathematically, the difference in power received by the two halves of the thermopile from targets whose images completely cover the thermopile areas is given by:

$$\Delta\phi = \frac{\sigma h w A}{\pi f^2} \left(\overline{T}_1^4 - \overline{T}_2^4\right) \text{ watts}, \qquad (1)$$

[6] *Harris, Louis, Final Report on the Development of Fast Response Thermopiles, Navy Dept. BuShips Contract NObs 25391, December 1946*

where $\Delta\phi$ = net power in watts,
σ = Stefan-Boltzman constant, 5.72×10^{-12} watts cm^{-2} deg^{-4},
h = height of thermopile in cm,
w = width of thermopile in cm,
A = cross-sectional area of the aperture of the optical system in cm^2,
π = 3.1416,
f = focal length of optical system in cm, and
$\bar{T}_1$, $\bar{T}_2$ = apparent radiation temperatures of targets in °K (as modified by the emissivities of the targets and atmospheric absorption).

If one half the thermopile is covered and maintained at a temperature, T_O, the power, ϕ, incident upon the exposed half is:

$$\phi = \frac{\sigma\, hwA}{\pi f^2} (\bar{T}_1^4 - T_0^4) \text{ watts} \quad (2)$$

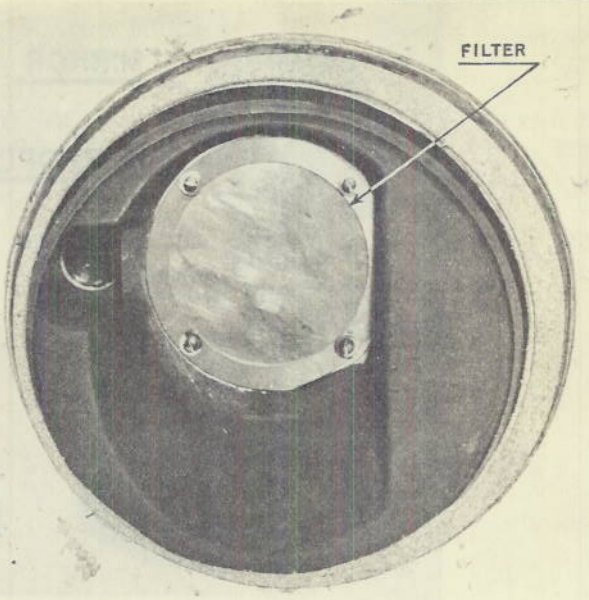

Figure 3 - Exterior view of mounting in observation window

From this last expression the apparent radiation temperature, $\bar{T}_1$, of a sky background is obtainable by measuring simultaneously, ϕ with one half the thermopile covered and the ambient temperature, T_O, of the covered half. For this purpose a metal slip-on "half-mask" was employed to cover one half of the thermopile, and a thermometer with the bulb

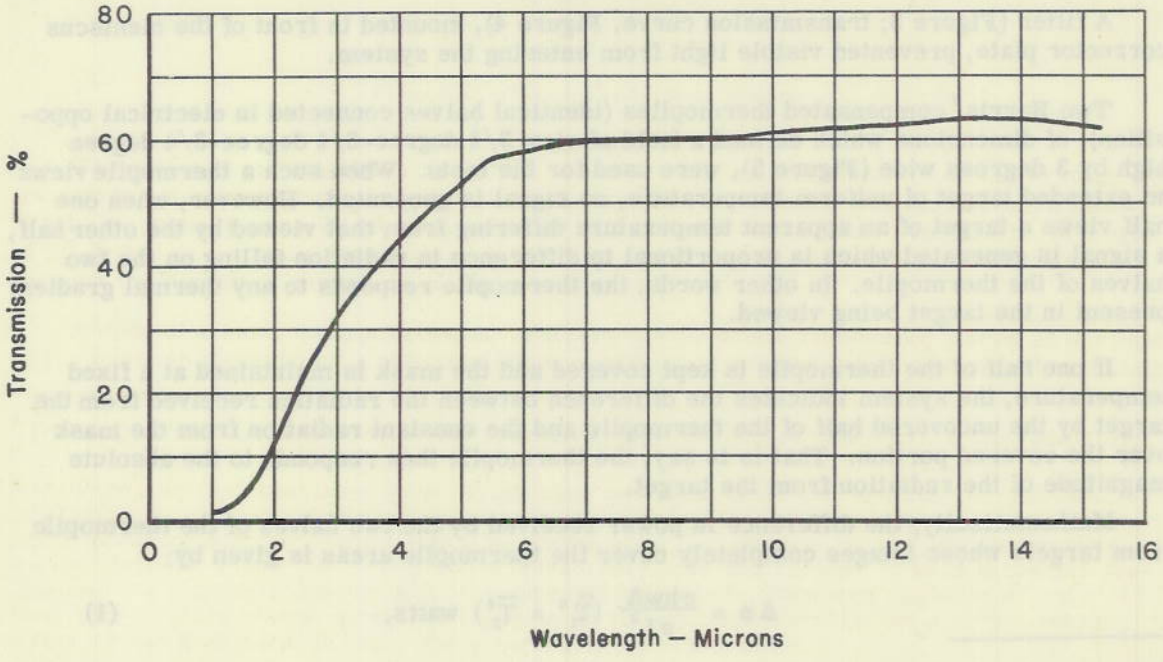

Figure 4 - Transmission of radiation filter

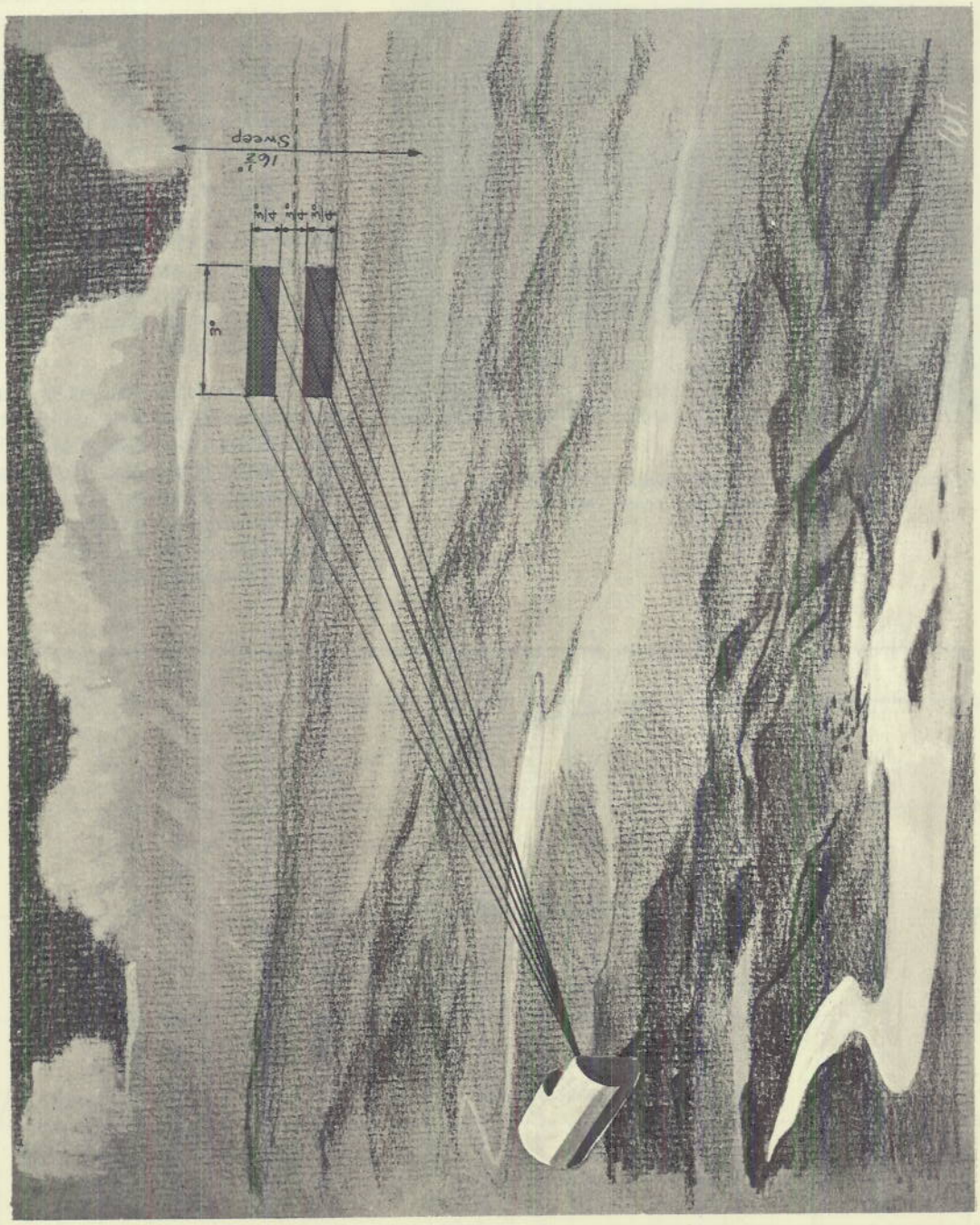

Figure 5 - Projected optical field of view

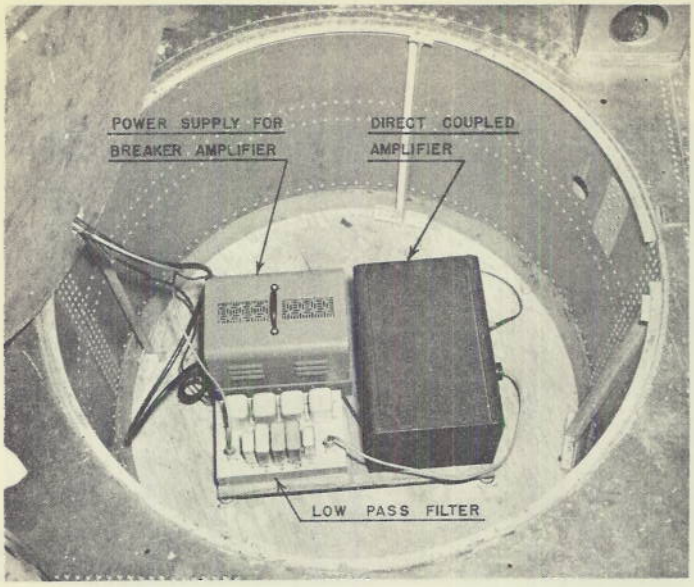

Figure 6 - Filter, direct-coupled amplifier, and breaker amplifier power supply

projecting into the optical system was employed to give ambient temperature readings. To eliminate drift errors caused by spurious thermal junctions in the thermopile leads, a blackened metal slide, which covered the thermopile completely, was inserted to "zero" the system before taking readings. Thereafter, the slide was removed.

The signal voltages generated by the thermopile were fed into a Model 53 Perkin-Elmer d-c breaker-type amplifier whose input impedance matched the d-c resistance (approximately 25 ohms) of the thermopile.

To remove the breaker "hash" present in the output from this type of amplifier, the voltage was filtered with a low-pass filter (Figure 6) whose characteristics (Figure 7) were chosen to provide good transmission for all types of signals encountered.

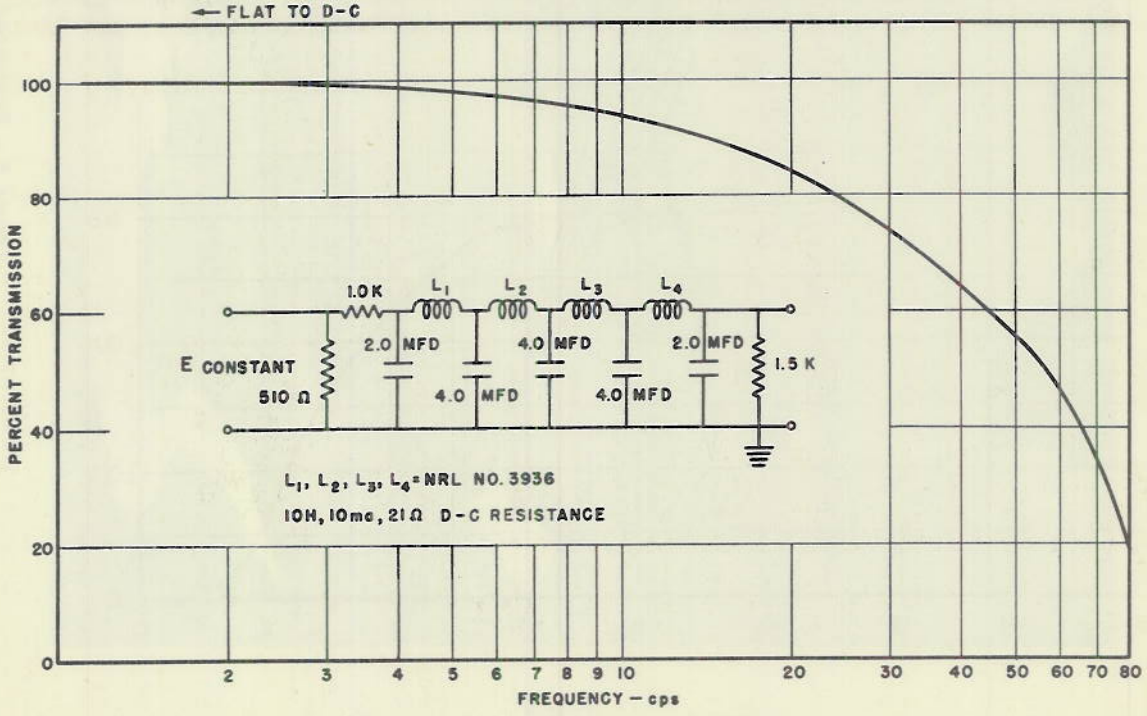

Figure 7 - Characteristics of the low-pass filter

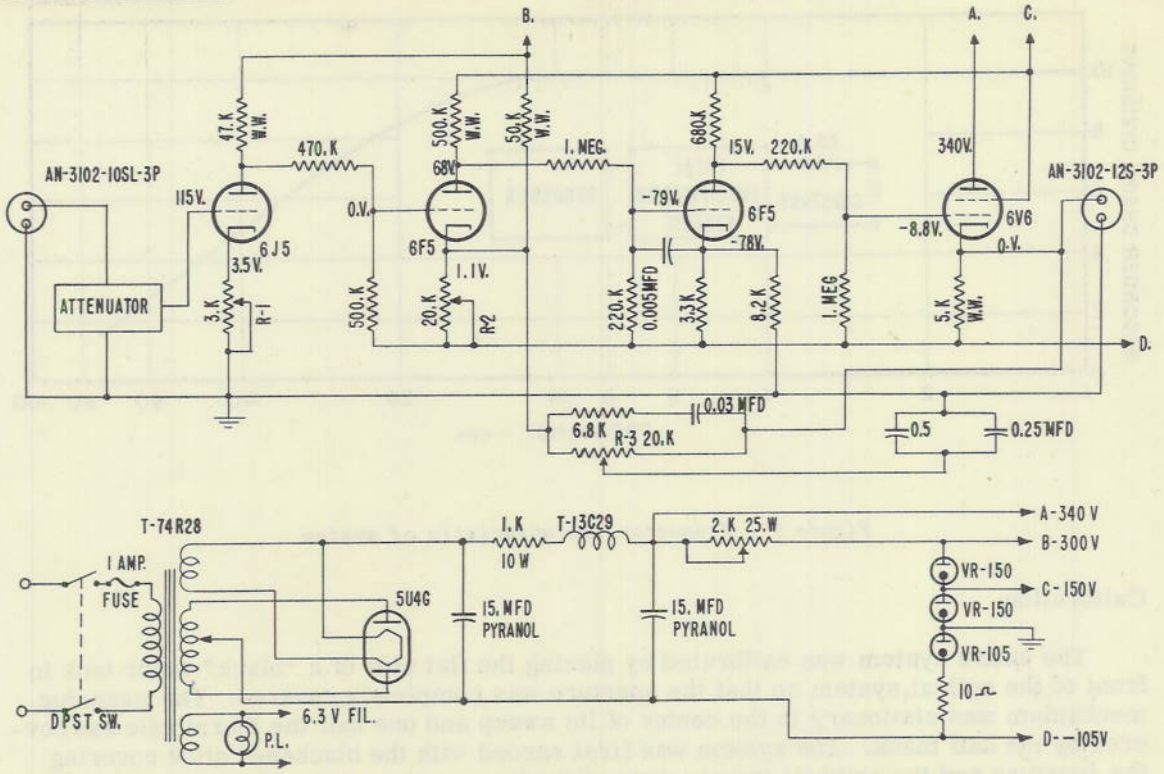

Figure 8 - Wiring diagram, direct-coupled amplifier

The signal was further amplified by the direct-coupled amplifier (Figure 6). This amplifier (circuit diagram, Figure 8), a modified version of the Brush Model 913 d-c amplifier, has a maximum voltage gain of 18 when employed with a 1500-ohm galvanometer element such as used in the Brush Model BL-202 recorder.

The direct-coupled amplifier drove one channel of a Model BL-202 Brush 2-channel recorder. With the aid of the negative feedback loop in the amplifier, the combined response of amplifier and recorder was made uniform out to 80 cps and hence did not appreciably alter the over-all frequency characteristics (Figure 9) of the entire system. The second channel of the recorder, connected to a switch operated by a cam on the scanner shaft, indicated the direction of travel of the scanner, as well as the beginning and end of each sweep.

Although from time to time during the actual measurements it was necessary to change the gain of amplifier system, a nominal over-all voltage gain of approximately 2×10^6 was employed in most cases. This corresponds to a system sensitivity of approximately 0.2 v/μ w measured at the input to the recorder.

A special converter already installed in the aircraft supplied the power for the entire system from a 115-volt, 60-cps line with a current drain of 4.5 amperes. The voltage and frequency regulation were good and no trouble was experienced from line transients.

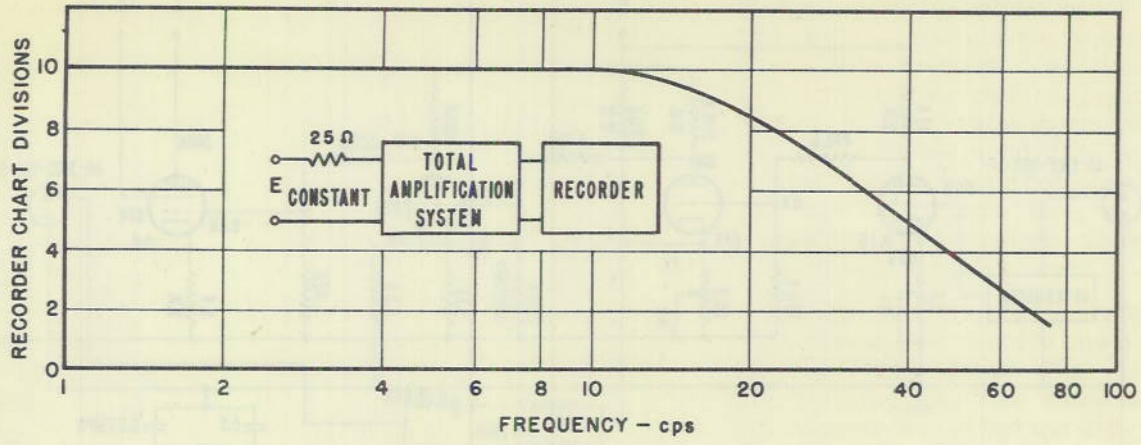

Figure 9 - Frequency characteristic of system

Calibration

The entire system was calibrated by placing the flat side of a "black" water tank in front of the optical system so that the aperture was completely covered. The scanning mechanism was stationary in the center of its sweep and one half the thermopile was covered by the half mask. The system was first zeroed with the blackened slide covering the aperture and the ambient temperature of the thermopile noted. The slide was then removed and readings taken as the temperature of the water was varied in 5-degree steps between room temperature and the boiling point of the water. The resulting recorder deflections were expressed in terms of an internal calibrating signal (inserted into the input of the breaker amplifier in series with the thermopile) equivalent to the open-circuit voltage of the thermopile, and graduated in steps of 0.1, 1.0, 10, and 100 microvolts.* By expressing all signals in terms of this calibrating voltage, the necessity of knowing the gain of the amplifying system or any variations therein is eliminated.

Having obtained the microvolt output from the thermopile as a function of the water temperature, and knowing the ambient temperature of the thermopile, an expression similar to (2) is employed to obtain the radiant power entering the system. Thus,

$$\phi = \frac{\sigma h w A}{\pi f^2} \quad (T_W^4 - T_O^4),$$

where
ϕ = effective radiant input power entering optical system,
$\sigma = 5.72 \times 10^{-12}$ watts $cm^{-2}\,deg^{-4}$,
h, w = height and width of thermopile area in cm,
A = cross-sectional area of aperture in cm^2,
$\pi = 3.1416$,
f = focal length of system in cm,
T_W = temperature of water in ^{0}K, and
T_O = ambient temperature of the thermopile in ^{0}K.

This is the same calibrating signal employed during the actual measurements.

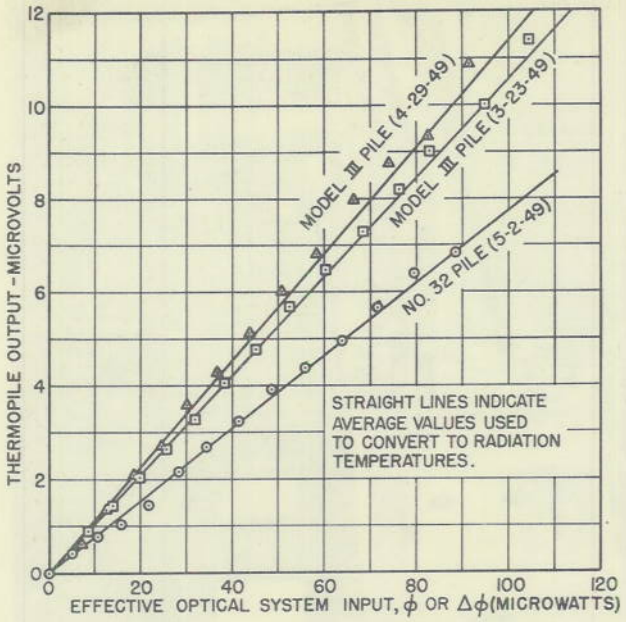

Figure 10 - Calibration curves

Actually the surfaces of the hot water tank, the half-mask, and the thermopile are not perfectly "black," but the error is less than 10% and can be neglected.

The resulting calibration curves for two different thermopiles are shown in Figure 10. Since the system is linear, the curves represent the deflections obtained with either one or both halves of the thermopile exposed.

Measurements obtained in flight, and expressed in terms of the thermopile's open-circuit voltage in microvolts, were converted to ϕ and $\Delta\phi$ by using the calibration curves of Figure 10. The apparent radiation temperature of the sky was then obtained using expression (2). Thermal gradient measurements have been left in terms of net power, $\Delta\phi$.

Installation

The equipment was installed in the B-29 aircraft as shown in Figures 6, 11, and 12. To eliminate troublesome effects from exhaust gases, the special mount to hold the scanning head was located ahead of the engines in a forward starboard port, and the window of the port was removed (Figures 11 and 12).

All units except the scanner were mounted on vibration-isolation mounts. The mounts employed were undersize and consequently were overloaded and greatly extended with the result that their natural frequency of vibration was considerably reduced. This method of mounting, together with the fact that the signals encountered were relatively large, resulted in no interference whatsoever from vibrational noise.

An additional precaution which also helped was to minimize the effects of motion in the earth's magnetic field by employing, between the thermopile and the breaker amplifier, a special cable (type W-1861 of the Tensolite Corporation, New York) consisting of four separately insulated conductors tightly twisted (twelve turns per inch) and covered with copper braid and glass fibre insulation. By electrical connection of diagonally opposite conductors, fairly good symmetry in the earth's magnetic field is achieved, and the resulting induced emf's are held at a minimum.

The breaker amplifier and recorder were mounted together and secured on top of the aircraft's radio transmitter (Figure 11). The low-pass filter, the direct-coupled amplifier, and the power supply for the breaker amplifier (Figure 6) were secured to the floor of the "well" formed by the closed-off forward belly gun turret.

TEST PROCEDURE

A short time before each flight, while the aircraft was stationary on the ground, the equipment was checked by allowing it to scan across the horizon. Once the plane was in the air, the

following items were observed and recorded: (1) the absolute power, ϕ, received from the sky and land background, expressed in terms of the open circuit voltage of the thermopile; (2) the thermal gradients, $\Delta\phi$, present in the background, also expressed in terms of the open circuit voltage of the thermopile; (3) the ambient temperature, T_O, of the thermopile; (4) the cloud, haze, and general sky conditions; (5) the position of the sun; (6) the time; (7) the altitude of the aircraft; and (8) the heading of the aircraft.

The radiation measurement procedure involved first covering up the thermopile with the blackened slide and then "zeroing" the system. The slide was then removed and the optical system was allowed to scan the sky and land background. The resulting recorder deflections yielded a measure of the thermal gradient, $\Delta\phi$. The blackened slide was then replaced and the calibrating voltage, corresponding to the open circuit of the thermopile, inserted. From the resulting recorder deflection, the magnitude of the thermal gradient in microvolts could then be determined.

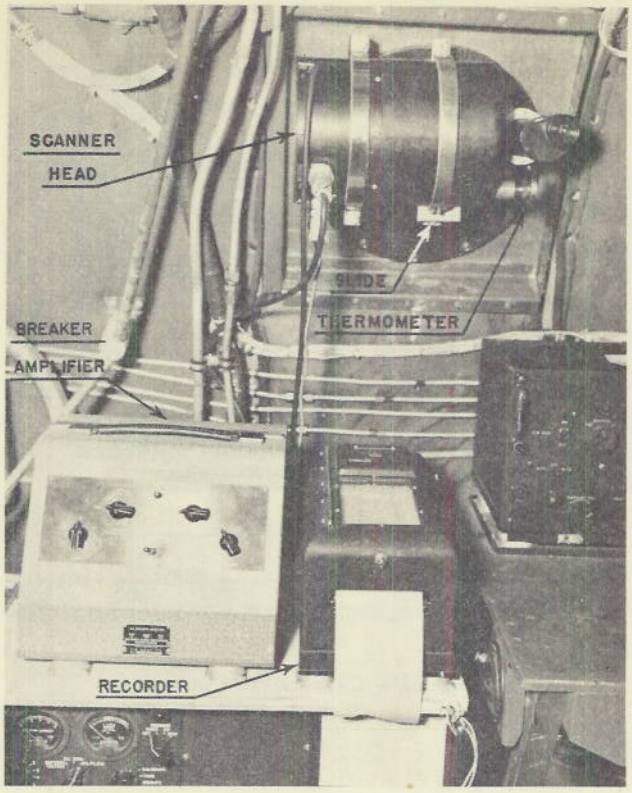

Figure 11 - Scanner head, breaker amplifier, and recorder

Immediately thereafter, the half-mask was placed over one half the thermopile and the system was again "zeroed" with the blackened slide in place. At this time the ambient temperature, T_O, of the thermopile was noted (usually $+8^{\circ}C$, compared with $-30^{\circ}C$ to $-40^{\circ}C$ for the outside air). The blackened slide was then removed and the system was allowed to scan across the background with the half-mask still in place. The resulting recorder deflection provided a measure of the absolute radiation, ϕ, from the background. The blackened slide was then replaced and the calibrating voltage switched in. From this recorder deflection, the magnitude of the absolute radiation, ϕ, in microvolts was determined.

Figure 12 - Location of optical system

After some experimentation with various flight plans, it was found that the best results were obtained by flying at a fixed altitude, with a fixed heading, and with the roll of the aircraft held to a minimum. This procedure was followed for all flights made. Although some records were made at other altitudes for comparison purposes, the constant altitudes flown were 30,000 with one unsuccessful attempt at 36,000 feet.

At the termination of the flight, the values of ϕ and $\Delta\phi$, in microvolts, were converted to watts using the calibration curves of Figure 10. The radiation temperature of the sky background was then determined from the values of ϕ and T_O inserted in equation (2).

RESULTS

Ground Measurements

A number of measurements were made on the ground at Armitage Field (Air Facility for NOTS, Inyokern) with the equipment installed in the plane. The optical system was permitted to scan across the horizon and both the absolute radiation and the thermal radiation gradients of the background were observed. Typical recordings are shown in Figure 13. The length and direction of one sweep of the optical system is indicated by the topmost trace. Recordings of absolute radiation and thermal radiation gradient are shown immediately below the reference trace.

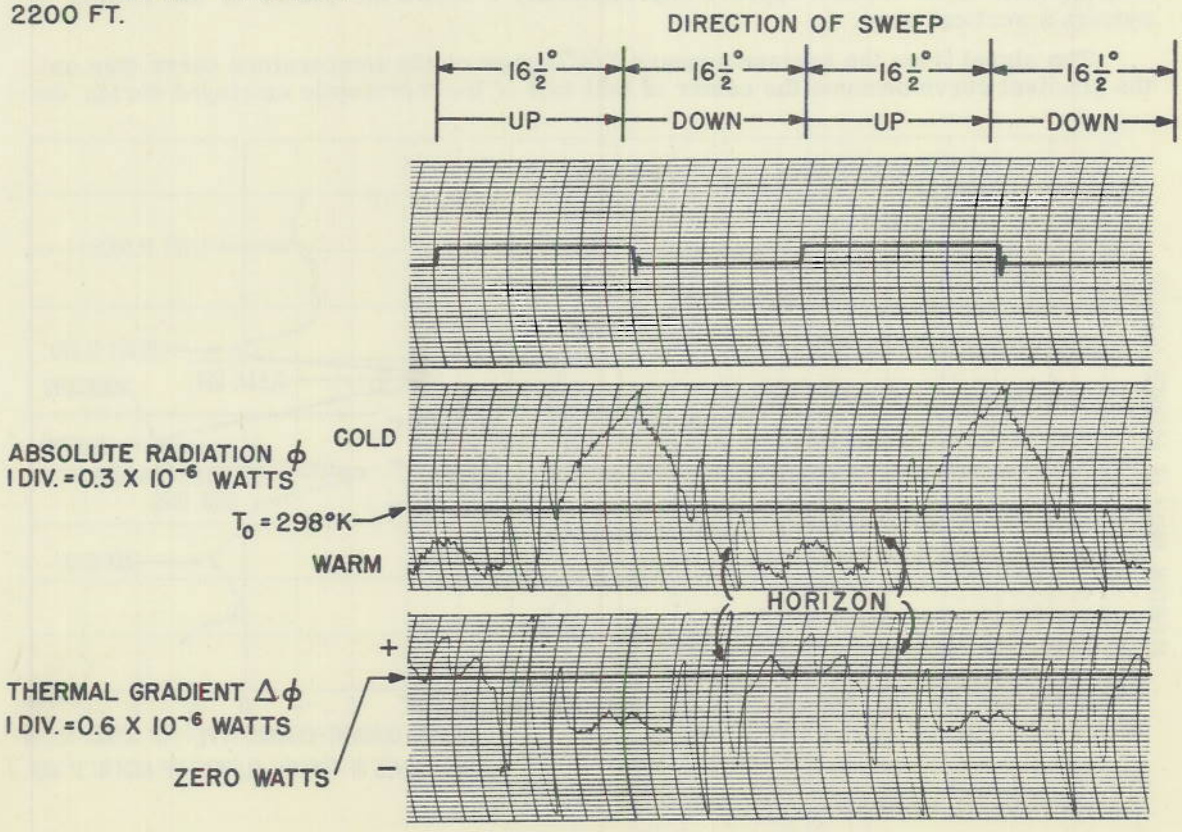

Figure 13 - Absolute radiation and thermal gradient observed from the ground

Both types of measurements could not be made simultaneously. Radiation gradient measurements were made first. Then the half-mask was placed in position over one half the thermopile and the absolute radiation measurements were made. Of course, if the two sets of measurements had been made simultaneously, a thermal radiation gradient curve would represent the approximate slope of an absolute radiation curve. But a period of approximately 8 minutes usually elapsed between the two sets of readings, and in the meantime, cloud movements altered the thermal radiation characteristics of the background and thus presented a different scene to the observer. Consequently, the thermal radiation gradient curves are only slightly related to the absolute radiation curves.

From the curves of Figure 13, the apparent radiation temperatures and the thermal radiation gradients have been plotted in Figure 14 as a function of the vertical angle of tilt of the optical system. The radiation temperature is expressed in degrees Kelvin and the radiation gradient in microwatts as observed directly with the two halves (3/4° high x 3° wide) of the thermopile separated $1\frac{1}{2}^{\circ}$ between centers.

Marked on each curve with a broken line is the position of the horizon as determined visually with the monocular whose optical axis was aligned with the optical axis of the scanner when the latter was in the middle of its vertical scan. Because of the tilt of the installation in the aircraft, the optical axis of the system when in the middle of its vertical scan was not horizontal but was tilted upward about $1\frac{1}{2}^{\circ}$. This was true for all the subsequent measurements. In addition, the horizon, which consisted of a mountain range 7 miles off, was approximately $\frac{1}{2}^{\circ}$ above the horizontal. Thus, as a net result of these displacements, the horizon appears approximately 1° below the center of the optical system's vertical scan.

The signal from the horizon appears 3/4° higher on the temperature curve than on the gradient curve because the center of that half of the thermopile employed during the

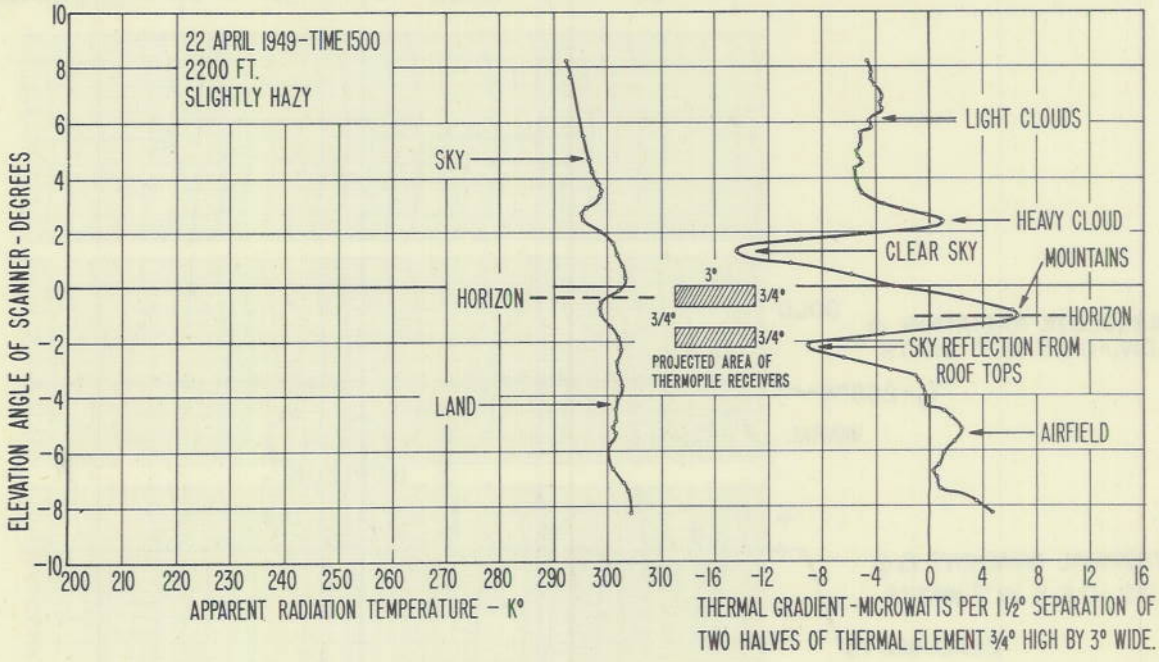

Figure 14 - Radiation temperatures and thermal radiation gradients in vicinity of horizon observed near sea level (2200 feet) during daytime

absolute radiation measurements lay 3/4° above the optical axis. Hence, when the exposed half of the thermopile was "looking at" the horizon, the optical axis of the system was actually 3/4° above the horizon. When both halves of the thermopile were exposed during the gradient measurements, the maximum signal from the horizon occurred when the horizon's image was midway between the two halves of the thermopile. In other words, the optical axis was right at the horizon.

It is quite apparent from Figure 14 that the position of the horizon can be determined readily from the thermal radiation gradient characteristics of the background. The gradient characteristic, however, exhibits a number of irregularities which could easily be mistaken for the horizon. At the extreme height of the vertical scan (+8°) both halves of the thermopile viewed light cirro-cumulus clouds. As the optical system swung downward, they encountered the edge of a dense cloud layer and gave a "getting warmer" indication. They then swung off the cloud layer onto a clear patch of sky and gave a "getting colder" indication. From there they crossed the horizon formed by mountain tops and produced a "getting warmer" indication. Next they encountered at the base of the mountain range some buildings with tin roofs from which sky radiation was reflected, thus producing a "getting colder" indication. Finally, the optical system swung down onto the airfield, and the thermopiles produced a "getting warmer" indication. No other major indication followed. It is thus apparent that the top edges of clouds or cloud layers produce signals of the same magnitude and polarity as the horizon.†

Airborne Measurements

The first airborne measurements were made on 22 April 1949. Take-off time was 0930. The aircraft climbed to 30,000 feet and then flew a straight course between San Diego and El Centro, California, at constant altitude. The weather was generally clear with scattered cloud layers in various locations and at many levels, some as high as 50,000 feet. In some cases, haze occupied the space between the bottom of the cloud and the ground, and in other areas this space was moderately clear. The topography was generally mountainous, with series of ranges extending to the horizon, as depicted in Figure 3. The flight was terminated at 1430. During this series of measurements, the sun was 40° or more above the horizon (never shining directly into the instrument) and hence contributed radiation only as the result of multiple reflection and scattering from haze, clouds, and the earth.

Typical recordings of absolute radiation and thermal radiation gradients in the vicinity of the horizon are shown in Figure 15, the absolute radiation curve having been obtained approximately 8 minutes after the thermal radiation curve. Because of the forward velocity of the aircraft, the background scene changed rapidly‡; hence the absolute and gradient curves represent totally different background scenes and are, consequently, only remotely related. It was noted that the residual roll of the aircraft while on autopilot also caused the position of the characteristic signals to shift along the time axis of the scanner.

From the recording of Figure 15, the apparent radiation temperatures and thermal radiation gradients of the background have been plotted (Figure 16) against the vertical angle of scan of the optical system. The position of the horizon, as determined with the aid of the monocular, is shown on the curves as a dotted line. It appeared approximately

---

†*This was also true at higher altitudes.*

‡*It should be noted that minor changes in the thermal radiation gradient curve occur with successive scans.*

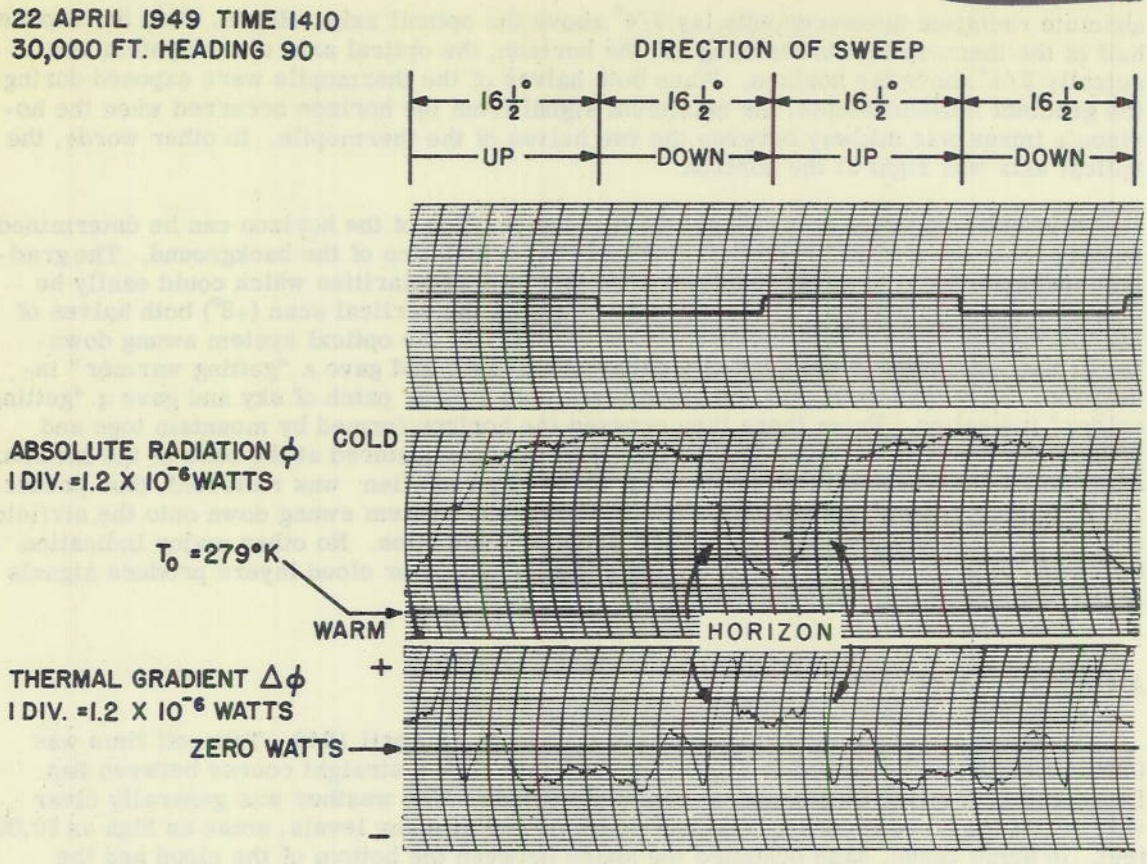

Figure 15 - Absolute radiation and thermal gradient observed at 30,000 feet

4° below the center of the vertical sweep of the optical system. Of this, $1\frac{1}{2}^0$ is due to the tilt of the installation in the aircraft and approximately $2\frac{10}{2}^0$ is due to the depression of the horizon[7] viewed from 30,000 feet.

A comparison of Figures 14 and 16 shows that the apparent radiation temperature of the sky was less at 30,000 feet than at sea level (2200 feet) and that it decreased faster with the upward tilt of the optical system at 30,000 feet than at sea level (2200 feet). An explanation is found in the fact that the sky appears "warmer" at low altitudes than at high altitudes because of the greater effective thickness of the atmospheric blanket between the receiver and outer space. Furthermore, when the receiver is tilted upward (Figure 17), the optical path length through the atmosphere does not decrease as fast at low altitudes as at high altitudes. Hence the radiation temperature of a low-altitude sky increases more slowly with the upward tilt of the optical system than does the radiation temperature of a high-altitude sky.

The thermal radiation gradients observed from 30,000 feet (Figure 16) exhibit the same general characteristics as those observed from near sea level (Figure 14). A large thermal radiation gradient existed at the horizon indicating the presence of a thermal

[7] *Humphreys, W. J., Physics of the Air, p. 469, 3rd Edition, 1940*

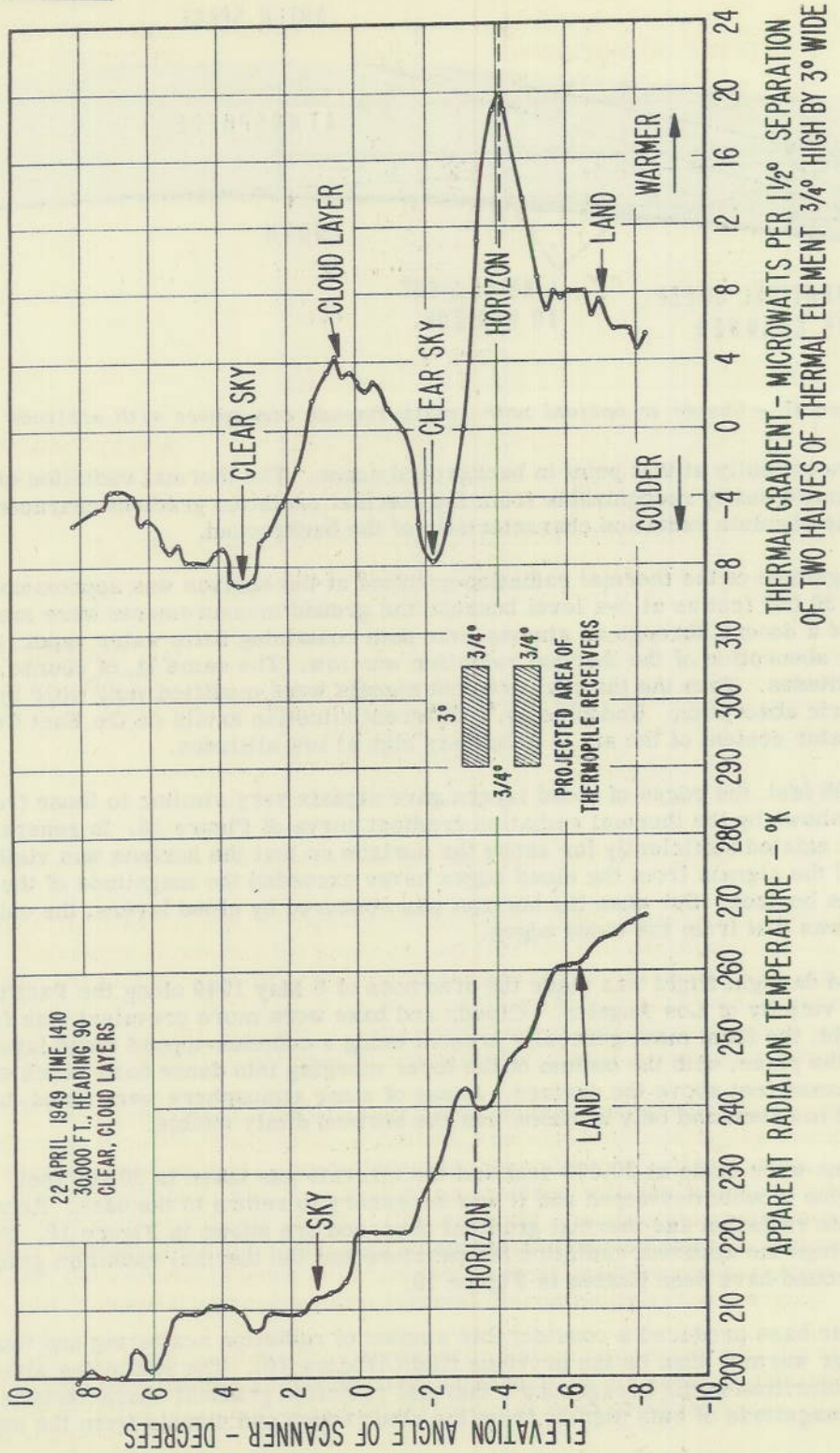

Figure 16 – Radiation temperatures and thermal radiation gradients in vicinity of horizon observed from 30,000 feet during daytime

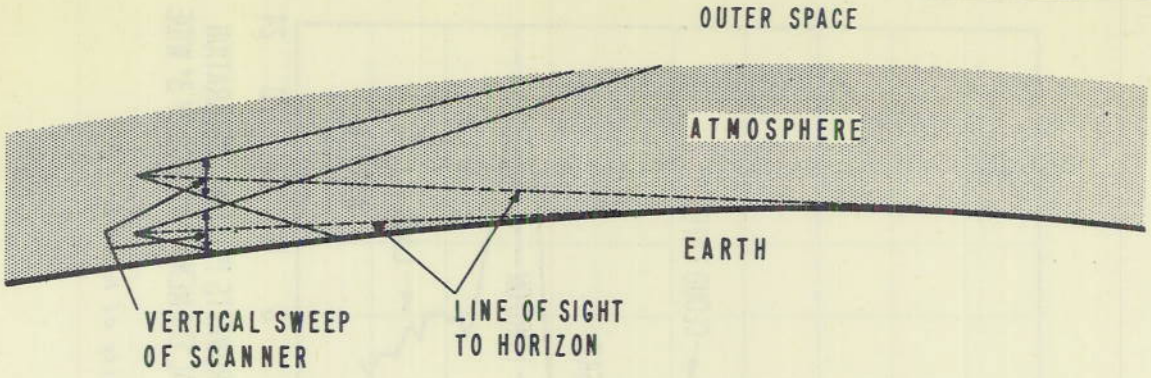

Figure 17 – Change in optical path length through atmosphere with altitude

radiation discontinuity at that point in background scene. The thermal radiation discontinuity was more easily recognizable from the thermal radiation gradient characteristic than from the absolute radiation characteristic of the background.

The magnitude of the thermal radiation gradient at the horizon was approximately the same at 30,000 feet as at sea level because the ground measurements were made in the middle of a desert, through an atmospheric path containing little water vapor, and the atmospheric absorption of the thermal radiation was low. The same is, of course, true at higher altitudes. Thus the thermal gradient signals were modified very little by changes in atmospheric absorption. Undoubtedly, a different situation exists on the East Coast where the water content of the air is relatively high at low altitudes.

At 30,000 feet, the edges of cloud layers gave signals very similar to those from the horizon, as shown by the thermal radiation gradient curve of Figure 16. In general, when cloud layers existed sufficiently far above the horizon so that the horizon was visible, the magnitude of the signals from the cloud edges never exceeded the magnitude of the signals from the horizon. But when the horizon was obscured by cloud layers, the only signal present was that from the cloud edges.

A second daylight flight was made the afternoon of 6 May 1949 along the Pacific Coast in the vicinity of Los Angeles. Clouds and haze were more prevalent than for the 22 April flight, the form most generally present being a cumulus-topped cloud layer at the level of the plane, with the bottom of the layer merging into dense haze which extended to a few thousand feet above the surface. Areas of clear atmosphere were found, but they were limited in extent and only at times was the horizon dimly visible.

Four runs were made at 30,000 feet and the aircraft was taken to 36,000 feet. During this run, engine trouble developed and it was necessary to return to the base. Recordings of the absolute radiation and thermal gradient observed are shown in Figure 18. From these recordings the apparent radiation temperature and the thermal radiation gradient of the background have been plotted in Figure 19.

The dense haze produced a considerable amount of radiation scattering and thus made the sky appear warmer than on the previous flight (Figure 16). The scattering also smoothed out the irregularities in the background's thermal radiation gradient characteristic and reduced the magnitude of both signals from the cloud edges and signals from the horizon.

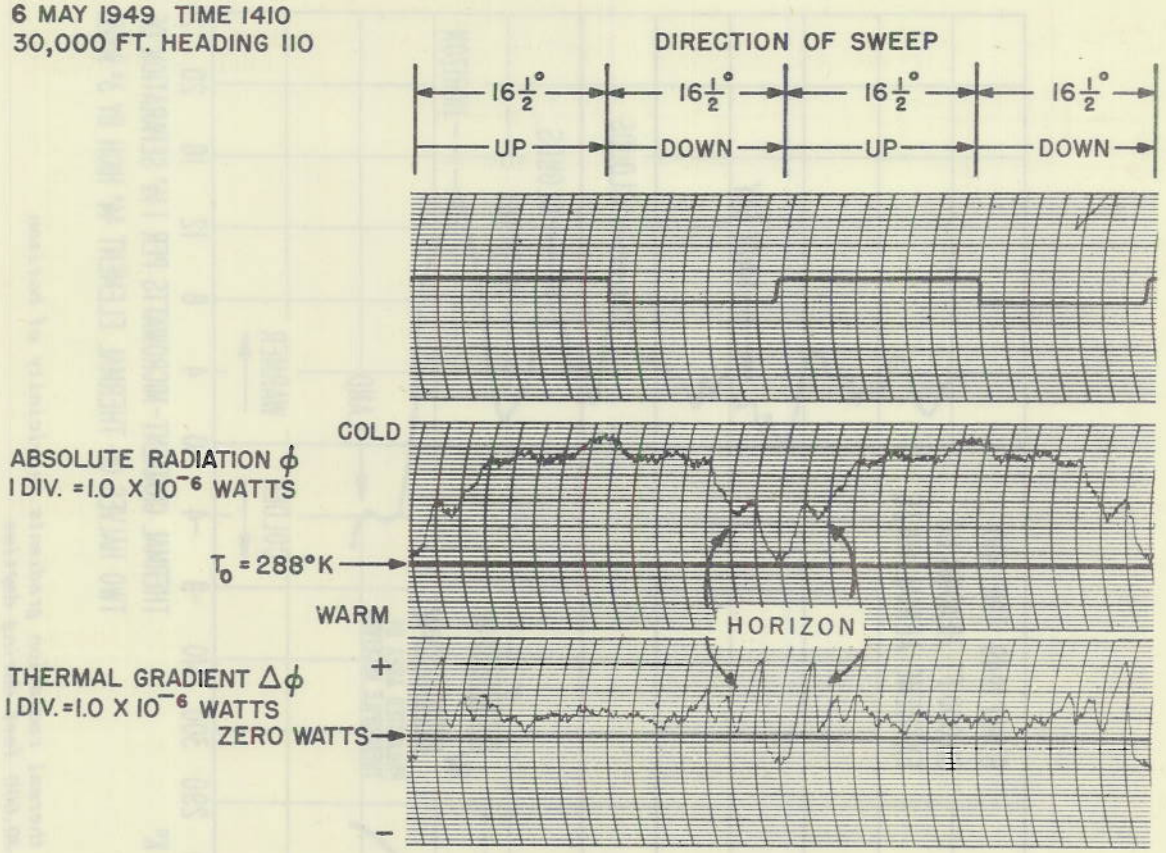

Figure 18 - Absolute radiation and thermal gradient observed at 30,000 feet

A third flight was made the night of 27-28 April, 1949, the takeoff being just after sunset. The course flown was the same as that for the first daytime flight—a line connecting San Diego and El Centro, California (essentially east-west). The stars were easily visible, and the outline of the horizon masking off the stars was discernible. Many clouds, varying in density and extent, were encountered directly in the path of, and near, the aircraft. This condition resulted in considerable modification of the received signals.

During this flight, that half of the thermopile which was covered during the absolute radiation measurements, and which, of course, was employed during the thermal gradient measurements, was damaged, it is believed by thermal shock and vibration. The result was that the damaged half, which normally was matched with the other half within 4%, suffered a reduction in sensitivity of 90%. Consequently, the absolute radiation measurements were unaffected but the thermal gradient measurements were in serious error. Nonetheless, the records (Figure 20) from the thermal gradient measurement, although in error, still showed the presence of a thermal discontinuity at the horizon.

In Figure 21, there is plotted the apparent radiation temperature of the night sky as calculated from the absolute radiation curve of Figure 20. In general, the thermal radiation characteristics of a night sky at 30,000 feet are similar to those of a day sky at the same altitude.

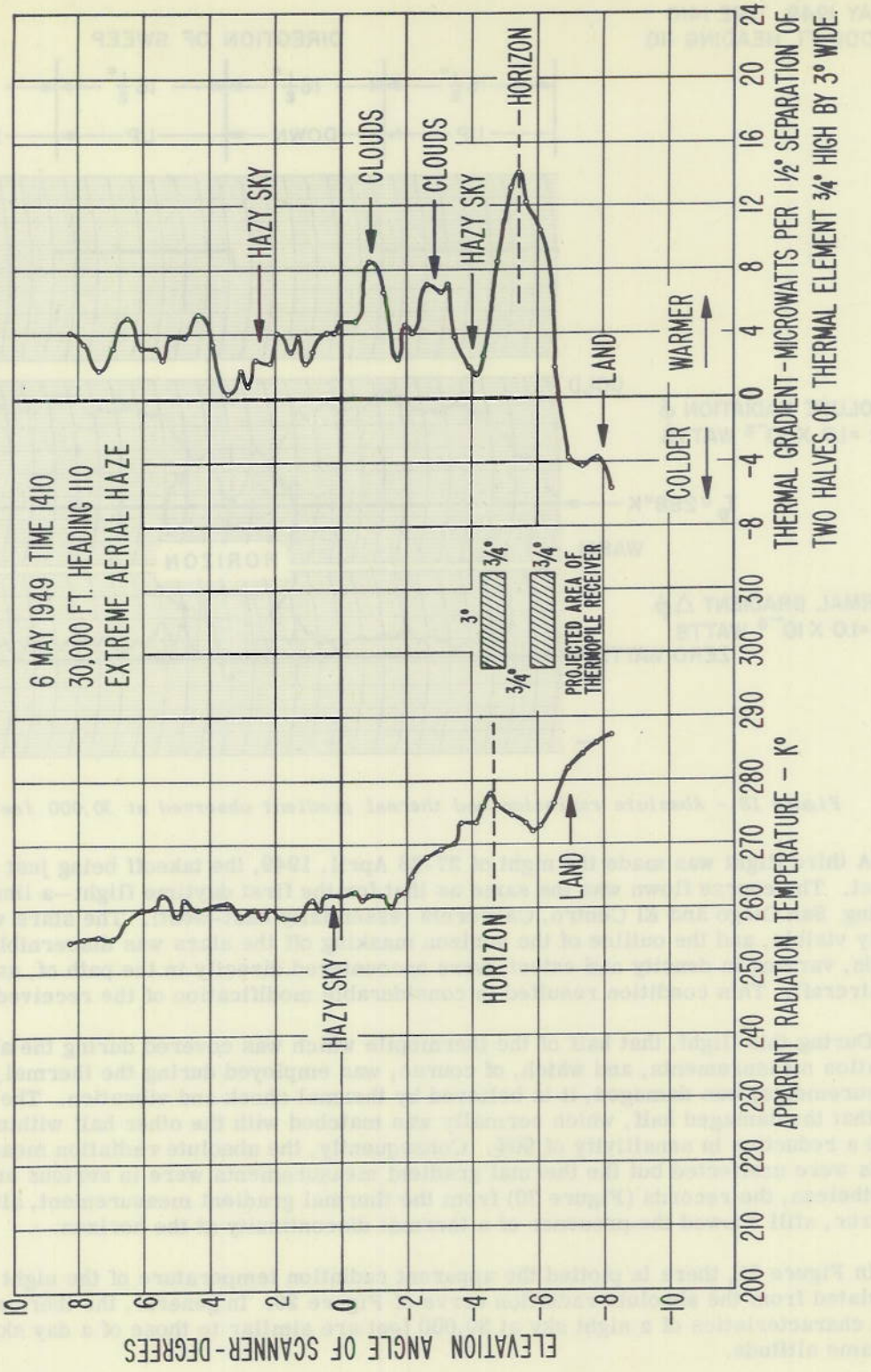

Figure 19 - Radiation temperatures and thermal radiation gradients in vicinity of horizon observed from 30,000 feet during daytime

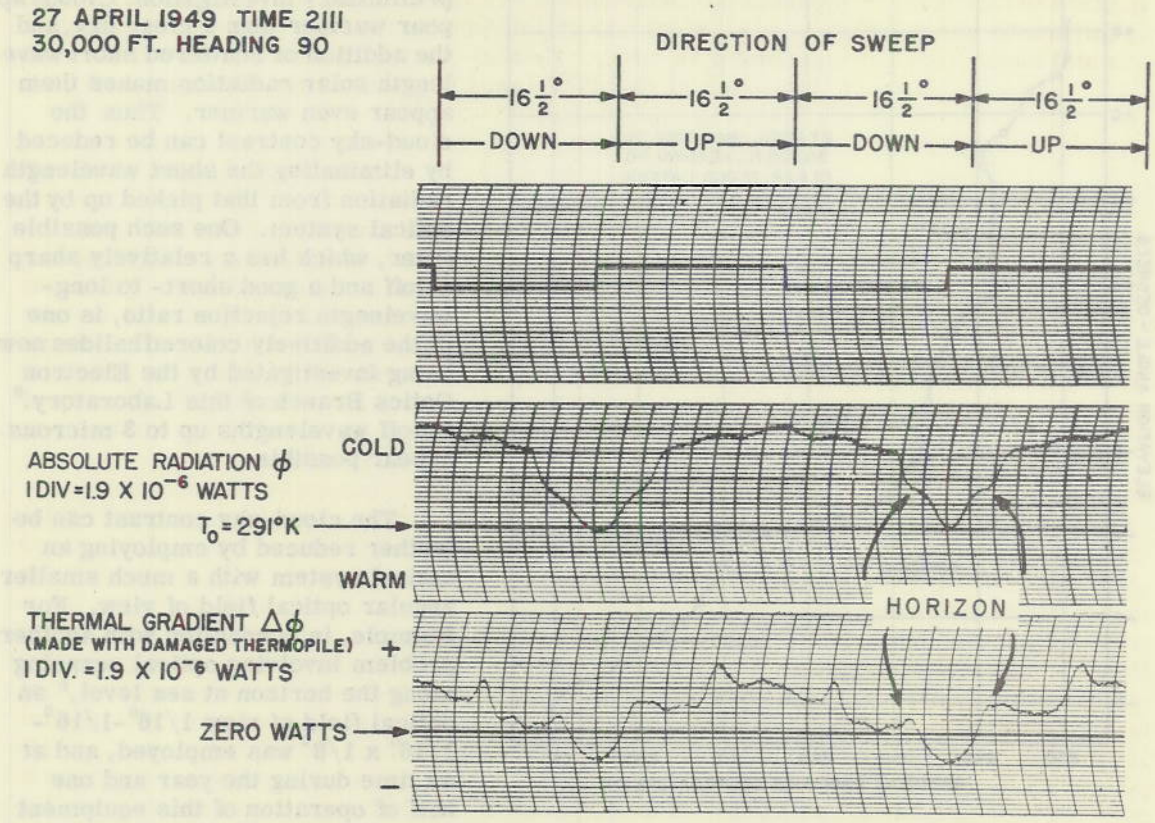

Figure 20 - Absolute radiation and thermal gradient observed at 30,000 feet at night

Cloud Interference

Clouds, usually just above the horizon, were encountered during all measurements. Thus, as the optical system swept downward, the clouds and then the horizon were picked up. The signal generated by crossing the edge of a cloud was often very similar in shape and of the same magnitude as the signal generated by crossing the horizon (Figures 16 and 19). Since clouds of this type were observed extending above the horizon in distinct layers to about 50,000 feet, any guidance system deriving its vertical from the horizon and used in a craft flying at altitudes as high as 10 times this altitude will confuse the edges of clouds with the horizon.

The problem is thus one of minimizing the cloud interference. If the signals from the clouds can be reduced to the point where they are never more than approximately one quarter the magnitude of the signal from the horizon, conventional electronic circuitry can provide the necessary discrimination. A poorer signal-to-noise ratio can be tolerated if it is permissable to average the signal over a sufficient period of time. An investigation of the thermal radiation characteristics of cloud edges must therefore be undertaken.

Because during the day the scattering of solar radiation is much more intense within clouds than in a clear sky, it will be necessary to obtain an optical filter with short wavelength rejection characteristics better (Figure 4) than those of the filter employed in this

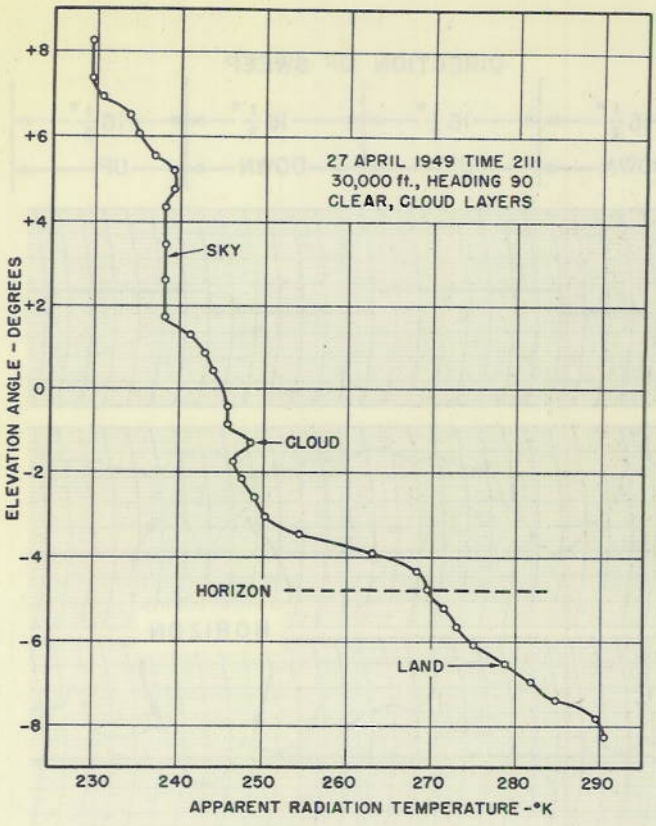

Figure 21 - Radiation temperature in vicinity of horizon observed at 30,000 feet at night

preliminary investigation. Clouds appear warmer than a clear sky, and the addition of scattered short wavelength solar radiation makes them appear even warmer. Thus the cloud-sky contrast can be reduced by eliminating the short wavelength radiation from that picked up by the optical system. One such possible filter, which has a relatively sharp cutoff and a good short- to long-wavelength rejection ratio, is one of the additively colored halides now being investigated by the Electron Optics Branch of this Laboratory.[8] Cutoff wavelengths up to 3 microns appear possible.

The cloud-sky contrast can be further reduced by employing an optical system with a much smaller angular optical field of view. For example, in connection with another problem involving optical scanning along the horizon at sea level,[9] an optical field of view $1/16^0$-$1/16^0$-$1/16^0 \times 1/8^0$ was employed, and at no time during the year and one half of operation of this equipment was cloud interference observed although other equipments with larger fields of view were affected. The minimum detectable power of this equipment was 0.2 microwatts, which means that the cloud signals were less than 0.2 microwatts. The cloud signals (thermal gradients) observed during these preliminary airborne measurements were 100 times this value. These increased signals are due partly to the fact that the sky appears colder at 30,000 feet than at sea level and hence the cloud-sky contrast is greater.

A good portion of this increase in signal, however, is due to the grossness of the optical field of view ($3/4^0 \times 3^0$, compared with $1/16^0 \times 1/8^0$ for each half of the thermopile) of the receiver. Many clouds do not have infinite thermal gradients at their edges, but, to a receiver with a large optical field of view they do so appear. A receiver with a field of view small enough to permit an exact measure of the thermal microstructure of the cloud edges should be employed if cloud interference is to be reduced.

---

[8] *Friedman, H. and Glover, C. P., "The Optical Transmission of Additively Colored Alkali Halide Crystals in the Visible and Near Infrared," (A letter to the Editor) by H. Friedman and C. P. Glover, JOSA, September 1949*

[9] *Clark, H. L., "A Survey of Thermal Radiation from Surface Vessels, Part I," NRL Report H-2764 (Confidential), May 4, 1946*

If clouds lie low enough to obscure the horizon, the problem of locating the horizon becomes either very difficult or completely insoluble. The top edge of the obscuring cloud layer will then undoubtedly appear to the receiver as a horizon. In some cases this error may be acceptable, particularly if time averaging is employed.

Probable Angular Accuracy

It is difficult to estimate the angular accuracy with which the thermal radiation discontinuity at or near the horizon can be located with the equipment employed in these exploratory measurements. It appeared to be possible to locate, with an error which did not exceed $\pm 1^{\circ}$, the position of the discontinuity relative to the vertical or any other fixed reference. The accuracy depends upon the vertical resolving power of the optical system and upon the shape of the absolute radiation characteristic above and below the horizon. In general, the error is less for an optical system with good than for one with poor resolving power.

For example, in Figure 22(a) an idealized and simplified absolute radiation characteristic (ϕ curve) is plotted for the case in which the sky above the horizon is clear (solid curve) and for the case in which a cloud layer exists immediately above the horizon but does not obscure it (broken curve). The horizon discontinuity is assumed for simplicity to be infinitely narrow. If an optical system with relatively good resolving power (for example, one in which each half of the field of view is 0.1° high with a 0.1° separation between halves) is employed to obtain the location of the thermal radiation discontinuity at the horizon by measuring the thermal radiation gradient, the position of the discontinuity can be located fairly accurately by observing the angular position of the peak in the gradient curve. On the other hand, if the same procedure is employed with an optical system of relatively poor resolving power (for example, one where each half of the field of view is 1° high with a 1° separation between halves), large errors may be introduced in determining the true angular position of the radiation discontinuity.

In Figure 22(b) there have been plotted the radiation gradient curves, $\Delta\phi$, calculated for the absolute characteristic curve, ϕ, for the several assumed cases. The solid curve, for the case of a clear sky, shows that for the high-resolving thermal receiver the discontinuity at the horizon is very sharp. The broken curve applies to the case of the cloud bank appearing above the horizon. It can be seen that the cloud bank introduces a slow variation in gradient with altitude which does not overlap the sharp discontinuity at the horizon. The signal from the horizon discontinuity therefore can still be used in this case.

Figure 22(c) gives the gradient curves for the same pair of examples but for the receiver with a comparatively wide field of view. For the clear-sky case, the signal from the horizon discontinuity is much broader but can still be used if one is content with less precision in angle. However, when clouds are added, an error of the order of $\frac{1}{2}^{\circ}$ is introduced into the position of the signal from the horizon discontinuity, and the whole gradient curve becomes changed in such a way that the signal from the horizon discontinuity could easily be confused with the signal from the clouds. In other words, it is possible by use of a high-resolving thermal receiver to reduce greatly, and in many cases avoid completely interference by cloud layers, provided the horizon itself is not obscured by the clouds.

For optimum resolution it appears that the widths of the thermal element should be about equal to the space between them. The permissible length of the thermal element is determined by the extent of the roll, pitch, and yaw of the missile for which the system must still be operative. In case appreciable motion is expected, the lengths of the thermal element receivers must be approximately equal to their widths. Otherwise, during a

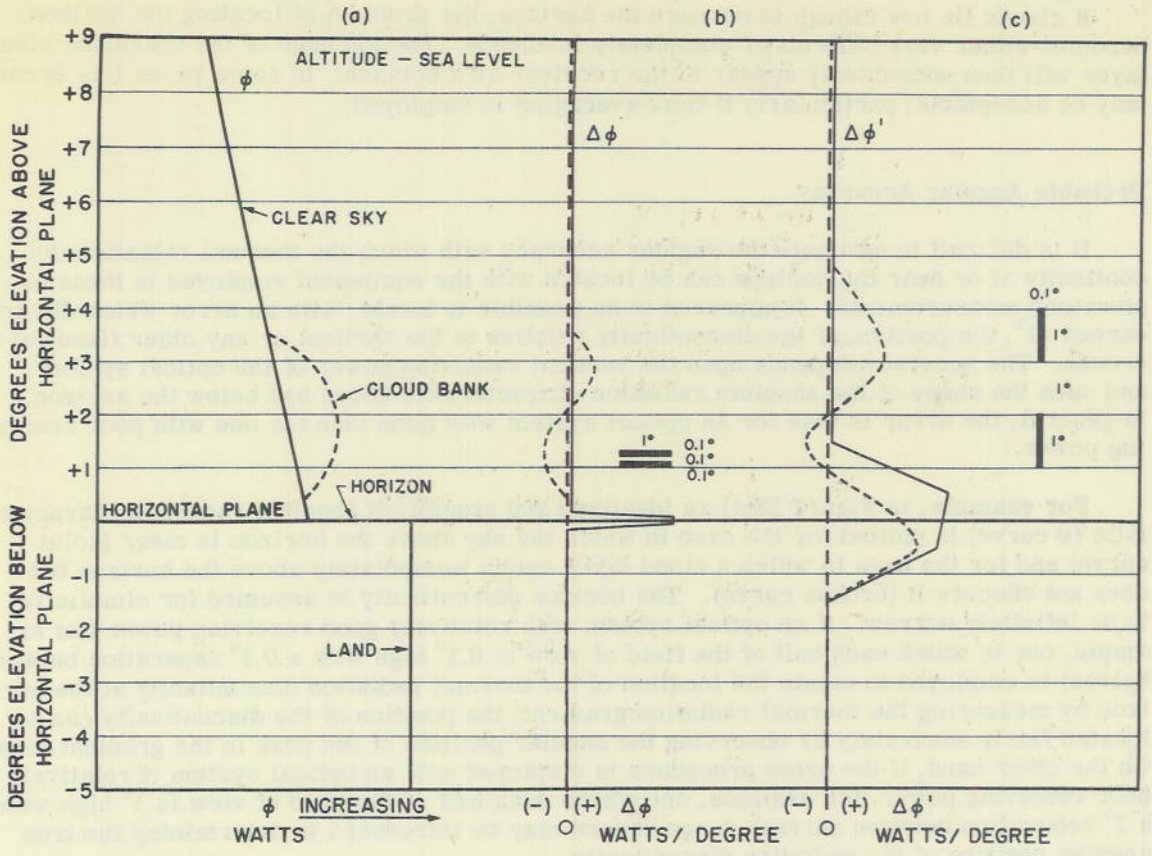

Figure 22 - Comparison of angular errors resulting from locating the horizon by means of gradient measuring devices with good and with poor resolving power

roll, for example, resolving power for the horizon discontinuity will be greatly reduced and the horizon may be completely obliterated.

It should be borne in mind that, in accordance with equation (1), any decrease in the dimensions of the optical field of view effected by reducing the size and spacing of the thermal element results in a decrease in the radiation differential, $\Delta\phi$, received by the system. Thus an optical system identical to the one employed for these exploratory measurements but with a 1 minute by 1 minute field of view will receive less than 1/8000th the radiation received by the exploratory system with its 3^0 x $3/4^0$ field of view under the same conditions. This difference is offset somewhat by the increased signal-to-noise ratio of the smaller element (increased sensitivity and decreased resistance due to reduction in linear dimensions). Nonetheless, such a reduction in signal will make the signal level at least 100 times smaller than the inherent electrical noise level of any practical missile-borne amplifying system. Hence a reduction in the dimensions of the optical field of view should be accompanied by little or no reduction in the signal-to-noise ratio of the over-all system. To reduce the optical field of view without suffering a loss in received radiation, it is necessary to increase the focal length and diameter of the optical system while maintaining the same f-number and leaving the linear dimension of the thermal elements unchanged.

SUMMARY AND CONCLUSIONS

1. A thermal radiation discontinuity existed at the horizon when observed at altitudes up to 30,000 feet.

2. A thermal radiation receiver which responds to thermal radiation gradients rather than to absolute radiation is best suited for observing the thermal radiation discontinuity at the horizon.

3. The accuracy with which the angular position of the thermal radiation discontinuity can be determined is limited by the resolution of the optical system employed. By making the vertical dimensions and the separation of each half of the optical field of view smaller, the accuracy can be increased. Under the conditions encountered in these experiments, the position of the horizon discontinuity relative to a fixed reference was located with an angular error which did not exceed $\pm 1^{0}$. Its constancy with elevation was not measured accurately.

4. In the geographical region in which the measurements were made, very little change was noted in the magnitude and characteristics of this thermal radiation discontinuity as the altitude of observation was increased.

5. The temperature of the sky appears colder at high altitudes than at sea level.

6. The apparent temperature of the sky decreases more rapidly with the elevation angle of the receiver at high altitudes than at sea level.

7. Cloud edges give signals very similar in shape and magnitude to those from the horizon when viewed with the optical receiver employed in these preliminary measurements.

8. It may be possible to reduce the interference from clouds if they lie above the horizon and do not obscure the horizon. If the horizon is obscured by clouds, the top edge of the obscuring layer may appear to the receiver as a horizon.

RECOMMENDATIONS

It is recommended that:

(1) Improved equipment be developed and measurements similar to these exploratory ones be repeated from a B-29 aircraft at 30,000 feet; the improved equipment incorporate such features as an improved optical filter and better optics; and efforts be made to employ an optical field of view as small as possible to reduce the cloud-sky contrast without reducing the land-sky contrast.

(2) The actual angular position of the thermal radiation discontinuity at the horizon be determined with greater accuracy relative to a true vertical at 30,000 feet in order to determine whether it is sufficiently constant in position to be of use in fixing the true vertical.

(3) Variations in the magnitude of the thermal radiation discontinuity and in its angular position be observed from high-flying aircraft under various weather and cloud conditions and at various geographical locations.

(4) Eventually, measurements also be undertaken from higher altitudes employing a vehicle such as the Skyhook balloon.

ACKNOWLEDGMENTS

The authors wish to express their appreciation for the cooperation extended the NRL group by the Upper Air Research Group at NOTS, Inyokern. They also wish to thank the Radiometry Branch, Optics Division of this Laboratory, for measuring the transmission of the radiation filter; Mr. C. T. Jeffrey for his part in constructing and testing the filter and direct-coupled amplifier; and Mr. C. R. Detwiler for his part in modifying, installing, and helping to operate the thermal detection gear.

* * *

NAVY-DPPO PRNC. WASH., D.C.